

EFFECTS OF GAS COMPOSITION ON ASYNCHRONOUS ERROR MOTION IN EXTERNALLY-PRESSURIZED SPINDLES

Michael W. Olson¹, David A. Arneson¹, Melvin J. Liebers¹, Eric R. Marsh²

¹Professional Instruments Co.

Hopkins, MN, USA

²Department of Mechanical Engineering

Penn State University

University Park, PA, USA

INTRODUCTION

Stable, externally-pressurized aerostatic spindles exhibit picometer-level vibration as a result of the interaction of the high pressure working fluid and its path through a spindle's compensation features (e.g., grooves, orifices, pockets, etc). This vibration presents a challenge as end users seek the lowest possible asynchronous error motion in manufacturing, metrology and data storage applications. This technical brief describes experimental testing to quantify this low-level vibration and its significant variation with both supply gas composition and pressure. Of the gases tested, helium and neon generate the lowest vibration while other gases including air lead to an order of magnitude higher vibration. Vibration levels with carbon dioxide and nitrous oxide are an additional order of magnitude higher. At present, the root cause of the vibration amplitude dependence on supply gas composition is unknown although kinematic viscosity and mean free path length correlate well with the results presented here.

BASELINE TESTING WITH AIR

Externally-pressurized spindles are nearly always used with air as the working gas. However, recent efforts to further reduce asynchronous error motion in ultra-precision spindle applications has led to exploration of other supply gases. As will be shown here, the working gas has a significant influence on the sub-nanometer background vibration, independent of manufacturer or compensation scheme in the spindles tested to date.

The first experiments presented in this brief are carried out on an unmotorized Professional Instruments ISO 3.25 spindle with groove compensation. A limited number of other manufacturers' spindles and compensation schemes were also tested with similar trends in results; in general, the RMS numbers vary from spindle to spindle but the trends remain the same. The spindle used in this

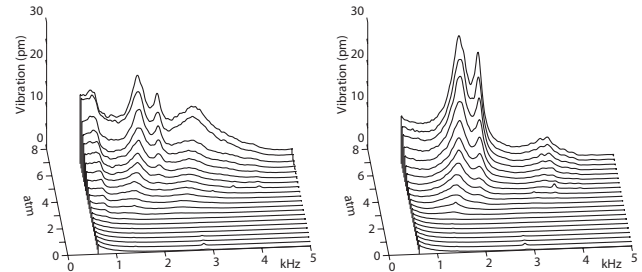


FIGURE 1. (a) Axial and (b) radial vibration in an externally-pressurized spindle with air as the working gas. The rigid-body response at lower frequencies is large because of the compliant support and is not plotted.

work is not installed in a machine, but rather rests on a compliant foam pad on an air isolation table. Temperature is controlled to $20 \pm 1^\circ\text{C}$ and the supply gases are drawn from cylinders. A single regulator was used to tap all gases using simple threaded adapters to accommodate the different bottle connector styles. This main regulator was left undisturbed in all testing at 10 atm. A second pressure regulator was used to adjust the pressure between 1 and 7 atm as needed. The same 2 m air line and fittings are used in all testing.

A high sensitivity triaxial accelerometer (1 V/g Kistler 8690C5) is fixed to the spindle rotor face plate to measure vibration in the axial and radial directions. Additional testing to quantify the compliance of the spindle as a function of gas type and supply pressure was performed with the same accelerometer and an instrumented hammer (2.25 mV/N Kistler 9722A500).

Baseline testing with air as the working gas shows an interesting trend in Figure 1. This figure shows the vibration spectra measured on the stationary spindle at different supply pressures from 0.3 to 7 atm in 0.3 atm increments. These water-

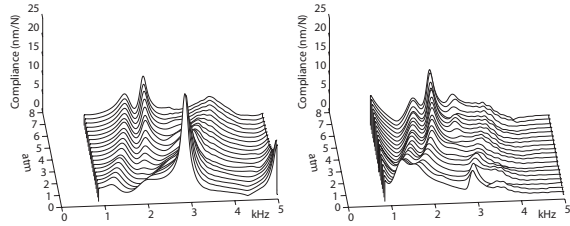


FIGURE 2. (a) Axial and (b) radial compliance of the spindle at increasing supply pressure (air).

fall plots are constructed from 21 separate tests with 500 averages each. At the lower supply pressures, the RMS vibration level in the frequency range of 400 to 5000 Hz is less than 1 pm. This is seen in the low amplitude spectra near the front of the waterfall plots. At higher air supply pressures, the RMS vibration increases monotonically to 11 pm at 7 atm. Because the individual spectral lines are obtained by twice integrating an accelerometer signal in the frequency domain by dividing by $(2\pi f)^2$, and because the spindle floats on a compliant support during testing, the lower frequencies do not provide relevant information and are removed for clarity.

In addition to the gradual rise in picometer-level vibration with the increasing supply pressure, Figure 1 also shows an increase in the three dominant natural frequencies in the 2 to 3 kHz range. This occurs because the stiffness of the air film increases with supply pressure while the inertia of the system remains constant. The stiffness increase is gradual because it is tempered by the increase in gas film thickness that results from elastic deformation of the spindle components under hydrostatic loading.

Figure 2 shows the measured dynamic compliance in the same 0.3 to 7 atm range of air supply pressure. Impact hammer testing requires measurement of an input (force) and an output (acceleration) on the spindle to compute the frequency response function characterizing the spindle dynamics. This figure more clearly shows the increase in natural frequencies that results from increasing air supply pressure because the resonant peaks are visible even at lower supply pressures. The modal damping values also change with supply pressure as evidenced by the amplitude of the resonant peaks. Interestingly, there is a supply pressure beyond which the overall dynamic compliance is no longer improved, presumably as a result of the hydrostatic pressure caus-

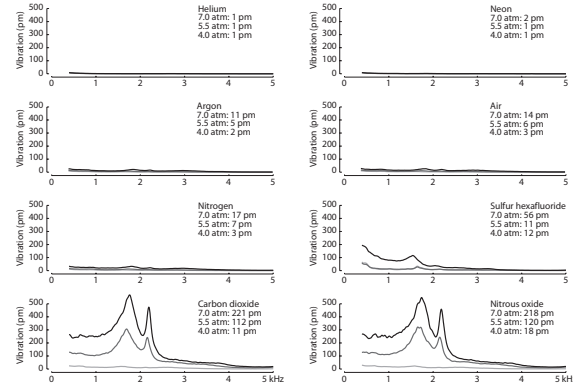


FIGURE 3. Ambient vibration levels from 400 to 5000 Hz for the eight tested gases.

ing increases in film thickness. Gas film stiffness varies with the third power of film thickness so even small changes can have a significant impact on performance.

RESULTS WITH OTHER WORKING GASES

The following results show that certain other working gases can significantly reduce the picometer-level vibration in a stable, externally-pressurized spindle. Seven additional gases are considered: helium (He), neon (Ne), argon (Ar), nitrogen (N_2), sulfur hexafluoride (SF_6), carbon dioxide (CO_2) and nitrous oxide (N_2O). These results are then compared to gas properties to look for possible correlation.

Figure 3 shows vibration levels measured on the same spindle with the eight different working gases. There is a large range of RMS vibration levels ranging from 1 pm for helium and neon to over 200 pm for nitrous oxide and carbon dioxide. Air is in between at 3 to 14 pm RMS, depending on the supply pressure. Another interesting feature of these measurements is the significant jump in vibration between supply pressures of 4 and 5.5 atm in carbon dioxide and nitrous oxide. This abrupt transition is not seen in the air results of Figure 1 so something is fundamentally different in these molecules that moves them into a different behavioral regime within the pressure range of interest.

Although it may not be practical to use neon or helium in most applications, the results suggest interesting physics governing the role of the supply gas composition in aerostatic spindle design. Insight into the influential characteristics of the lighter helium and neon might allow future spindle

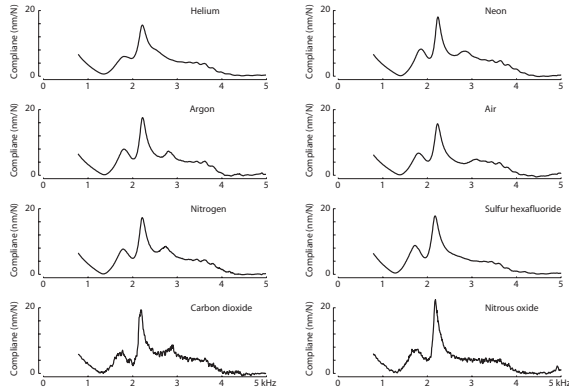


FIGURE 4. Axial compliance from 400 to 5000 Hz for the eight tested gases.

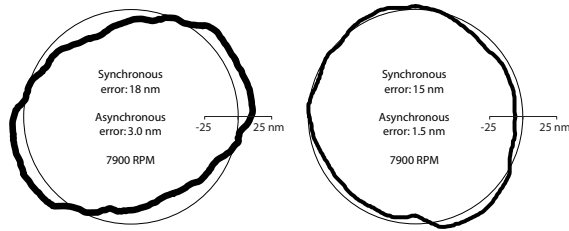


FIGURE 5. Radial error motion of two similar spindles run on air at 7900 RPM. The right-hand spindle has improved internal porting that halves the asynchronous error.

designs to be scaled to perform in a more desirable way.

The impact hammer test results of dynamic compliance with the same eight gases is much less variable, as shown in Figure 4. The tilt mode of vibration appears at frequencies ranging from 1770 Hz (SF_6) to 1900 Hz (Ne). The maximum value of the dynamic compliance of this resonance ranges from 4 to 5 nm/N. The small variation in amplitude does not correlate with the modal frequency. The axial mode ranges from 2170 Hz (SF_6) to 2230 Hz (Ne). The amplitude of this resonance ranges from 7 to 10 nm/N and also does not appear to follow any particular trend. For the most part, the measured variations in dynamic compliance are relatively small with supply gas. Since the same spindle is used in all testing (constant inertia), this suggests that the small changes in compliance are due to the effective stiffness and damping of the thin film of working gas and its interaction with the compensation of the spindle.

Gas	3.0 atm	5.5 atm	7.0 atm
	Asynchronous (nm)		
He	1	1	2
Ne	2	2	2
Ar	4	6	
Air	4	8	12
N_2	5	9	12
SF_6	6	7	10
CO_2	7	8	11
N_2O	10	12	15

TABLE 1. Asynchronous error motion of a spindle run at 7900 RPM with the eight gases.

Table 1 summarizes a second set of experiments to directly measure the most important quantity for many spindle applications: the asynchronous error motion, in this case measured at 7900 RPM. These results were obtained using an entirely different setup; here the spindle is hard-mounted on a sturdy test bench. A reversal is not needed because we are only concerned with the asynchronous component. Figure 5 shows two representative polar plots of radial error motion from testing of two similar spindles with air as the working gas.

The error motion measurement is made using a capacitive sensor (Lion Precision DMT-22 drivers and C1-C probes) scanning the equator of a lapped spherical artifact (Professional Instruments) that is rigidly bolted to the spindle chuck. The roundness of the lapped artifact is better than 12 nm at the equator. The test data are collected using software and data acquisition equipment from Lion Precision (SEA system). The noise floor of the spindle error measurement is approximately 1 nm. As seen in Table 1 the asynchronous error of the spindle on helium is at or below the noise floor of the measurement. Table 1 also shows that the asynchronous component is quite low for neon and is larger for the remaining gases. The overall increasing trend in asynchronous error motion matches the results from earlier static vibration testing (Figure 3).

At 7 atm, helium provides a six-fold decrease in asynchronous error motion compared to air. This improvement is smaller than the differences seen in static vibration testing, with some of the discrepancy likely due to masking of the true asynchronous error motion in helium by noise. In any event, helium and neon give remarkably better (ie, lower) asynchronous error motion compared to air. This large improvement would be of par-

Gas	Molecular weight g/mol	Kinematic viscosity mm ² /s	Molecular diameter pm	Mean free path (STP) nm
He	4.0	110	258	196
Ne	20.2	35	279	140
Ar	39.9	13	342	72
Air	29.0	14	330	68
N ₂	28.0	14	375	67
SF ₆	146.1	2	551	25
CO ₂	44.0	7	390	45
N ₂ O	44.0	7	388	39

TABLE 2. A few properties of the gases tested in this research.

tical interest in storage applications where the synchronous error motion is mapped out leaving only asynchronous error motion to limit the track pitch. Asynchronous error motion also limits the achievable surface finish in single point turning.

At present, no single explanation has emerged for the observed trends. However, two figures of merit that correlate well to the increase in vibration and asynchronous error motion are the Reynolds number and the mean free path of the gas molecules. These and other material properties are summarized in Table 2.

The kinematic viscosity appears in the Reynolds number Re which is used to predict the transition to turbulence.

$$Re = \frac{v L}{\nu}$$

where:

- v = fluid velocity
- L = characteristic length
- ν = kinematic viscosity

The apparent Reynolds number resulting from the rotation of a spindle, even at high speeds, is small because the fluid film thickness is so thin. However, the Reynolds number associated with the exhausting high pressure gas is generally much higher. A representative Reynolds number is difficult to calculate because of the uncertainty in identifying the appropriate fluid velocity and characteristic geometric feature inside a compensated spindle. However, the kinematic viscosity will appear in the denominator for each calculation to directly affect the results. The correlation coefficient R^2 of the Reynolds number to the measured

asynchronous error motion is 0.6. The helium results stand out slightly from the observed trend, most likely because the true asynchronous error motion using helium is at or below the noise floor of the experimental setup.

The mean free path l is the average distance the gas molecules travel between collisions with other molecules.

$$l = (n\sigma)^{-1}$$

where:

- n = number of particles per unit volume
- σ = effective cross sectional area for collision

The mean free path also correlates somewhat to the level of vibration in externally-pressurized gas spindles. The correlation coefficient R^2 of the mean free path to the measured asynchronous error motion is 0.6 (0.8 if sulfur hexafluoride is excluded).

ACKNOWLEDGEMENTS

The authors gratefully acknowledge Mark Toffle of Minneapolis, MN for originally suggesting this investigation of the performance of air bearings spindles using other working gases. His insight motivated the work presented here.